Electromagnetic Field Analysis and Its Applications to Product Development

Tomohiro KEISHI

Electromagnetic field analysis, one of the numerical analysis, is now an indispensable method for designing and developing electromagnetic application products. Such advanced analysis techniques including finite element methods and faster, higher-capacity analytical hardware, such as personal computers, enable even the most complex electromagnetic phenomena to be investigated. Depending on the frequency of an object, an analysis is carried out differently; products with high frequency must be analyzed in the electromagnetic field, while products with relatively low frequency can be studied in the either field: the electric or magnetic field. This paper describes the outline and purposes of the electromagnetic field analysis, introducing some examples of the experiment.

Keywords: electromagnetic field analysis, electric field analysis, magnetic field analysis, finite element method, product design

1. Introduction

Numerical electromagnetic field analysis has become an essential tool for the design and development of electromagnetic products [(1)-(16)]. Advances in numerical analysis techniques, including the finite element method and high-speed, high-capacity analytical hardware such as the personal computer have made it possible to investigate numerically even the most complex electromagnetic phenomena. The frequencies involved in the operation of a product determine how the analysis must be carried out: in some cases, the electric field and magnetic field may be studied separately, as in electric field analysis and magnetic field analysis; while in other cases it is necessary to study both the electric and magnetic fields simultaneously, as in electromagnetic field analysis. This paper outlines and describes the purpose of electromagnetic field analysis, and presents examples of product design and development. The future outlook for electromagnetic field analysis is also discussed.

2. Electromagnetic Field Analysis

2-1 Fundamental Equations of Electromagnetic Field Analysis

The electromagnetic fields $\boldsymbol{E}$ and $\boldsymbol{B}$ that are produced by the electric current $\boldsymbol{i}$ and the electric charge q can be represented using Maxwell's equations (1)-(4), where Equation (1) is Faraday's law of electromagnetic induction, Equation (2) is Ampere's law with Maxwell's correction, Equation (3) is Gauss's law, and Equation (4) is Gauss's law for magnetism [(17)].

$$\mathrm{rot}\boldsymbol{E} = -\frac{\partial \boldsymbol{B}}{\partial t} \quad \cdots\cdots (1)$$

$$\mathrm{rot}\boldsymbol{B} = \mu_0 \boldsymbol{i} + \varepsilon_0 \mu_0 \frac{\partial \boldsymbol{E}}{\partial t} \quad \cdots\cdots (2)$$

$$\mathrm{div}\boldsymbol{E} = \frac{q}{\varepsilon_0} \quad \cdots\cdots (3)$$

$$\mathrm{div}\boldsymbol{B} = 0 \quad \cdots\cdots (4)$$

Here $\boldsymbol{E}$ is the electric field, $\boldsymbol{B}$ magnetic flux density, $\boldsymbol{i}$ current density, t time, q charge density, ε_0 permittivity in a vacuum, and μ_0 permeability in a vacuum.

Within a substance of permittivity ε and permeability μ, the following equations hold:

$$\boldsymbol{D} = \varepsilon \boldsymbol{E} \cdots\cdots (5)$$

$$\boldsymbol{B} = \mu \boldsymbol{H} \quad \cdots\cdots (6)$$

Hence, Equations (2) and (3) can be represented as Equations (2)' and (3)' [(17)].

$$\mathrm{rot}\boldsymbol{H} = \boldsymbol{i} + \frac{\partial \boldsymbol{D}}{\partial t} \quad \cdots\cdots (2)'$$

$$\mathrm{div}\boldsymbol{D} = q \cdots\cdots (3)'$$

Here, $\boldsymbol{D}$ is the electric flux density, and $\boldsymbol{H}$ is the magnetic field.

If the divergence of both sides of Equation (2)' is taken, div(rot$\boldsymbol{H}$)=0, and taking Equation (3)' into account, the law of conservation of charge (Equation (7)) may be deduced.

$$\mathrm{div}\boldsymbol{i} = -\frac{\partial q}{\partial t} \quad \cdots\cdots (7)$$

When dealing with a phenomenon in the high-frequency range, it is necessary to solve an electromagnetic field problem involving electric and magnetic fields at the same time. In this case, Maxwell's equations (1)-(4) or (1), (2)', (3)' and (4) must be solved.

When dealing with a phenomenon in the low-frequency range, on the other hand, it is often sufficient to solve either an electric field problem or a magnetic field problem. In this case, it is necessary to solve a quasi-static electromagnetic field equation relating to either the elec-

tric field or magnetic field (see **Table 1**).

When dealing with the electric field only, Equations (3)', (7), and (1)' in **Table 1**[17] may be solved.

From Equation (1)', the relation between $\boldsymbol{E}$ and electric potential V can be defined in Equation (8).

$$\boldsymbol{E} = -\,\mathrm{grad}\,V \quad \cdots\cdots(8)$$

If electrical conductivity σ or resistivity ρ are used, the relation between $\boldsymbol{i}$ and $\boldsymbol{E}$ is represented by Equation (9).

$$\boldsymbol{i} = \sigma\boldsymbol{E} = \frac{\boldsymbol{E}}{\rho} \quad \cdots\cdots(9)$$

When dealing with the magnetic field only, Equations (2)", (1), and (4) in **Table 1**[17] may be solved.

From Equation (4), the relation between $\boldsymbol{B}$ and vector potential $\boldsymbol{A}$ can be defined by Equation (10).

$$\boldsymbol{B} = \mathrm{rot}\boldsymbol{A} \quad \cdots\cdots(10)$$

Table 1. Maxwell's equations (Quasi-static electromagnetic field equations)

The electric field system		The magnetic field system	
$\mathrm{div}\boldsymbol{D} = q$	(3)'	$\mathrm{rot}H = \boldsymbol{i}$	(2)"
$\mathrm{div}\,\boldsymbol{i} = -\frac{\partial q}{\partial t}$	(7)	$\mathrm{rot}\,E = -\frac{\partial \boldsymbol{B}}{\partial t}$	(1)
$\mathrm{rot}\,E = 0$	(1)'	$\mathrm{div}\boldsymbol{B} = 0$	(4)
$E = -\mathrm{grad}V$	(8)	$\boldsymbol{B} = \mathrm{rot}\,\boldsymbol{A}$	(10)
$\boldsymbol{D} = \varepsilon E$	(5)	$\boldsymbol{B} = \mu H$	(6)
$\boldsymbol{i} = \sigma E = \frac{E}{\rho}$	(9)	$\boldsymbol{i} = \sigma E = \frac{E}{\rho}$	(9)

2-2 Electromagnetic Field Analysis Using Numerical Analysis

Several numerical techniques have been developed for electromagnetic field analysis. Among these, one of the most frequently chosen is the finite element method, as it is highly versatile and thus applicable to most problems [18]-[20].

As shown in **Table 1**, in the case of equations relating to the electric field, if the scalar potential V which satisfies $\boldsymbol{E} = -\,\mathrm{grad}\,V$ is introduced, $\mathrm{rot}\boldsymbol{E} = 0$ is identically satisfied. In the case of an electrostatic field problem, the time derivative of charge density q is zero. Since $\mathrm{div}\boldsymbol{i} = 0$, it is not necessary to solve this equation. Since $\mathrm{div}\boldsymbol{D} = \mathrm{q}$ and $\boldsymbol{D} = \varepsilon\boldsymbol{E} = -\varepsilon\,\mathrm{grad}\,V$, all that remains is to find the V that satisfies the Poisson's equation (11).

$$\mathrm{div}(\varepsilon\,\mathrm{grad}\,V) = -q \quad \cdots\cdots(11)$$

If $q = 0$, all that remains is to solve the Laplace's equation (12).

$$\mathrm{div}(\varepsilon\,\mathrm{grad}\,V) = 0 \quad \cdots\cdots(12)$$

As shown in **Table 1**, in the case of equations relating to the magnetic field, if the magnetic vector potential $\boldsymbol{A}$ which satisfies $\boldsymbol{B} = \mathrm{rot}\boldsymbol{A}$ is introduced, $\mathrm{div}\boldsymbol{B} = 0$ is identically satisfied. In the case of an electrostatic field problem, $\boldsymbol{B}$'s time derivative is zero and $\mathrm{rot}\boldsymbol{E} = 0$. Since $\mathrm{rot}\boldsymbol{H} = \boldsymbol{i}$ and $\boldsymbol{H} = \frac{1}{\mu}\boldsymbol{B} = \frac{1}{\mu}\mathrm{rot}\boldsymbol{A}$, all that remains is to find the $\boldsymbol{A}$ that satisfies Equation (13).

$$\mathrm{rot}\left(\frac{1}{\mu}\mathrm{rot}\boldsymbol{A}\right) = \boldsymbol{i} \quad \cdots\cdots(13)$$

In the case of a quasi-steady magnetic field problem, or an eddy current problem, both electric scalar potential ø and magnetic vector potential $\boldsymbol{A}$ are introduced to represent the electric field $\boldsymbol{E}$ and magnetic flux density $\boldsymbol{B}$ in Equations (14) and (15), respectively.

$$\boldsymbol{E} = -\,\mathrm{grad}ø - \frac{\partial \boldsymbol{A}}{\partial t} \quad \cdots\cdots(14)$$

$$\boldsymbol{B} = \mathrm{rot}\boldsymbol{A} \quad \cdots\cdots(15)$$

If Equations (14) and (15) are used, Equation (2)"can be represented in Equation (16), with Equations (6) and (9) also being taken into account.

$$\mathrm{rot}\left(\frac{1}{\mu}\mathrm{rot}\boldsymbol{A}\right) = \sigma\left(-\,\mathrm{grad}ø - \frac{\partial \boldsymbol{A}}{\partial t}\right) \quad \cdots\cdots(16)$$

Since $\mathrm{div}(\mathrm{rot}\boldsymbol{H})=0$, Equation (17) holds.

$$\mathrm{div}\left\{\sigma\left(-\,\mathrm{grad}ø - \frac{\partial \boldsymbol{A}}{\partial t}\right)\right\} = 0 \quad \cdots\cdots(17)$$

If Equations (16) and (17) are solved, a solution to the eddy current problem may be attained.

3. Electric Field Analysis

3-1 Purpose of Electric Field Analysis

Cables and coils are often used in electric power transmission circuits. High voltage is applied between internal and external conductors of the cable and between the coil conductor and the surface of an insulator, thereby placing a high electric field stress on the insulator. When the insulator is subject to excessive electric field stress, dielectric breakdown occurs, terminating the transmission of electric power. It is therefore necessary to determine the electric field accurately so as to design electrical insulation to include sufficient tolerance, avoiding excessive electric fields across the insulator. If, like cables, the insulator's cross section is circular, it is possible to determine the electric field through analysis. Because most insulators have a complex shape and more than one type of electrical insulator is used, however, it is necessary to conduct electric field analysis to determine the electric field.

3-2 Element Discretization to Determine the Maximum Electric Field

The finite element method was used for electric field analysis of a parallel plate electrode with a spheroid at its top (see **Fig. 1**) to determine the maximum electric field at the tip of the projection. The distance between the parallel plates is 3 mm, and a voltage of 50 Hz, 38 kV is ap-

plied. The major axis radius of the spheroid is 1,325 μm, and the radius of curvature at the tip is 50 μm. As shown in **Fig. 2 (a), (b), and (c)**, electric field analysis was conducted by alternating finite element discretization near the tip of the projection. Shown in **Fig. 3** is how the maximum electric field at the tip of the projection relates to the thickness of the element. If these three points are used to determine a quadratic regression line to approximate the maximum electric field, it is assumed to be 238.6 kV/mm (element thickness = 0 mm), with a theoretical value of 236.4 kV/mm [21]. With an error ratio of less than 1%, the value estimated from the finite element method and the theoretical value are in close agreement.

In this way, it is necessary to cut thin slices of the element at the point where the maximum electric field is calculated. The thickness of the element must be determined so that the required accuracy for the maximum electric field is achieved.

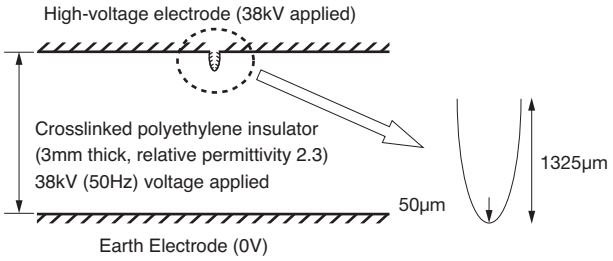

Fig. 1. Spheroid projection models

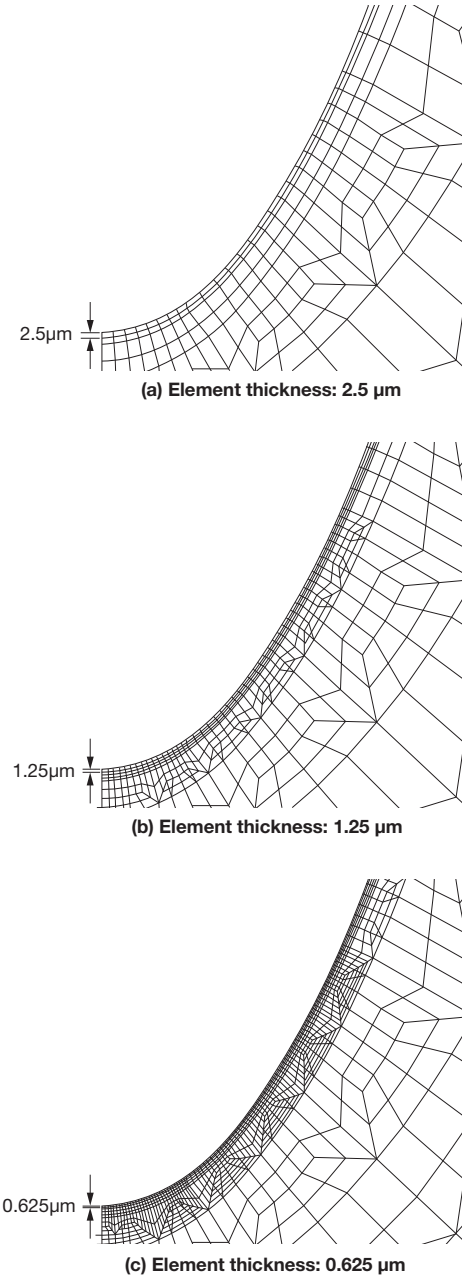

Fig. 2. Finite element discretization near the tip of the projection

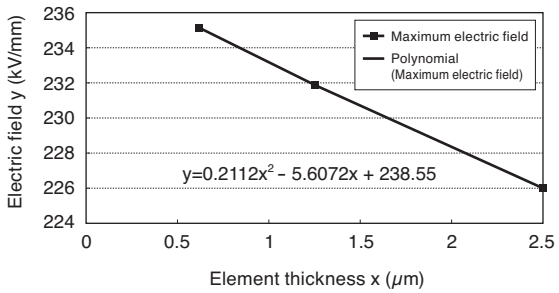

Fig. 3. Element thickness and maximum electric field at the tip of the projection

3-3 Designing Power Cable Equipment by Using Electric Field Analysis

In order to design power cable equipment, such as normal joints and sealing ends [22], three electric field analysis techniques (shown in **Table 2**) are required.

Electrostatic field analysis takes into account the insulator's permittivity, solely to find the electric field distribution. The voltage distribution in electrical power equipment that is operated with commercial alternating current (AC current of 50 Hz or 60 Hz) is determined by the permittivity. Since most power cables carry commercial alternating current, this analysis technique is most frequently used.

Complex electric field analysis takes into account both the insulator's permittivity and resistivity (or electrical conductivity) to find the electric field distribution. This technique is primarily used for electric field analysis of power cable equipment, the steepness of whose potential gradient is moderated with a semiconducting sleeve (shrinkable tube). This technique is also used to calculate the electric field distribution of an insulator to which three-phase current is applied, where it is necessary to consider the phase difference of each conductor's potential.

Direct electric field analysis takes into account resistivity (or electrical conductivity) only to calculate the electric field distribution. The voltage distribution of electric power equipment that is operated under direct current is determined by resistivity. This technique is primarily used for analysis of power cable equipment for direct current

Table 2. Electric field analysis for designing power cable equipment

Type	Physical properties considered	Linear / Nonlinear	Applications
Electrostatic field analysis	Relative permittivity ε_r	Linear analysis	AC electric cable equipment
Complex electric field analysis	Relative permittivity ε_r Resistivity ρ (electrical conductivity σ)	Linear analysis	AC electric cable equipment ·Equipment using semiconducting sleeves, etc. ·When the phase difference of three-phase alternating voltage is considered
Direct electric field analysis	Resistivity ρ (electrical conductivity σ)	Nonlinear analysis $\rho=\rho(E,T)$ E: Electric field, T: Temperature	Direct current electric cable equipment

submarine cables. In Japan, this technique was used for electric field analysis of the submarine cable connecting the Aomori prefecture on the main island (Honshu) to Hokkaido (Hokkaido-Honshu direct electric trunk cable) and the power cable equipment for the direct current 500-kV submarine cable connecting the Tokushima prefecture on the island of Shikoku to Honshu's Wakayama prefecture (Anan-Kihoku direct current trunk cable) [23].

The relation with Maxwell's equations concerning the electric field (**Table 1**) is assumed to be as follows [24]:

For an insulator whose permittivity is ε and volume resistivity is ρ, the following equations hold, where $\boldsymbol{E}$ is the electric field, $\boldsymbol{i}$ is the current density, and q is the space charge density.

$$\mathrm{div}(\varepsilon \boldsymbol{E}) = q \quad \cdots\cdots(18)$$

$$\mathrm{div}\, \boldsymbol{i} = \mathrm{div}\left(\frac{\boldsymbol{E}}{\rho}\right) = -\frac{\partial q}{\partial t} \quad \cdots\cdots(19)$$

Based on Equations (18) and (19), when ε is temporally constant,

$$\mathrm{div}\left(\frac{\boldsymbol{E}}{\rho} + \varepsilon\frac{\partial \boldsymbol{E}}{\partial t}\right) = 0 \quad \cdots\cdots(20)$$

For an alternating voltage of angular frequency ω, if complex numbers are used to represent stationary electric fields on the assumption that

$$\boldsymbol{E} = \hat{\boldsymbol{E}} = E_0\left\{\cos(\omega t+\phi)+j\sin(\omega t+\phi)\right\} = E_0 e^{\,j(\omega t+\phi)}$$

then Equation (20) would be:

$$\mathrm{div}\left\{\left(\frac{1}{\rho}+j\omega\varepsilon\right)\hat{\boldsymbol{E}}\right\} = 0 \cdots\cdots(21)$$

From Equation (21), the following three cases are assumed, depending on ε, ρ, and ω.

(1) High Frequency or Capacitance Fields

$$\left(\text{when } \frac{1}{\rho} << \omega\varepsilon, \text{ i.e., } \varepsilon\,\rho\,\omega >> 1\right)$$

$$\mathrm{div}\left(\varepsilon\hat{\boldsymbol{E}}\right) = 0 \cdots\cdots(22)$$

This equation represents a normal electrostatic field. The relative permittivity and resistivity values of an insulator used in power cable equipment are shown in **Table 3** [25),(26)]. If frequency f = 50 Hz, $\omega = 2\pi f$ = 314 rad/s. Then, if relative permittivity ε_r = 1 and resistivity $\rho = 10^{15}$ are assumed, the following equations hold:

$$1/\rho = 1/(10^{15}\times10^{-2}) = 10^{-13}(1/\Omega\mathrm{m})$$
$$\omega\varepsilon = 314\times1\times8.854\times10^{-12} = 2.78\times10^{-9}(1/\Omega\mathrm{m})$$

Thus $1/\rho << \omega\varepsilon$ is satisfied. Accordingly, in order to analyze the electric fields of power cable equipment operated at commercial frequencies, Equation (22) needs to be solved by taking only permittivity into account.

Table 3. Relative permittivity and volume resistivity of each insulating material

Materials	Relative permittivity	Volume resistivity (Ωcm)
Polyethylene	2.3	10^{18}
Crosslinked polyethylene	2.3	10^{18}
Polytetrafluoroethylene (Teflon)	2.0	10^{15}
Natural rubber	3-4	10^{15}
Butyl rubber	3-4.5	10^{15}
EP-rubber	4-5	10^{15}
Epoxy	3.5-5	10^{15}-10^{17}
Insulating paper	1.2-2.6	–
Impregnated paper (Oil-impregnated paper)	3.5-3.7	10^{18}
Insulating oil	2-5	10^{16}

Note: The above values may differ depending on the composition of each material. Care must be taken when using them for analysis.

(2) Direct Current or Low-resistance Fields

$$\left(\text{when } \frac{1}{\rho} >> \omega\varepsilon, \text{ i.e., } \varepsilon\,\rho\,\omega << 1\right)$$

$$\mathrm{div}\left(\frac{\hat{\boldsymbol{E}}}{\rho}\right) = 0 \quad \cdots\cdots(23)$$

This is the same as Equation (22), except that ε is replaced by $1/\rho$. In the case of direct current, frequency f = 0, and so $\omega\varepsilon$ = 0, thus satisfying $1/\rho >> \omega\varepsilon$. Therefore, it is necessary to solve Equation (23) by taking only resistivity into account in order to analyze the electric fields of power cable equipment operated with direct current.

(3) General Cases

Equation (21) is the same as the equation in which ordinary permittivity ε of equation (22) is replaced by complex permittivity $\hat{\varepsilon}$ of equation (24).

$$\hat{\varepsilon} = \varepsilon + \frac{1}{j\omega\rho} \quad \cdots\cdots (24)$$

In order to analyze the electric fields of power cable equipment the insulator resistivity of which is smaller than that in case (1) above and that are operated at commercial frequencies, it is necessary to use Equation (24) where both permittivity and resistivity are considered.

Shown in **Fig. 4** are types of electric field analysis to be used with resistivity and frequency.

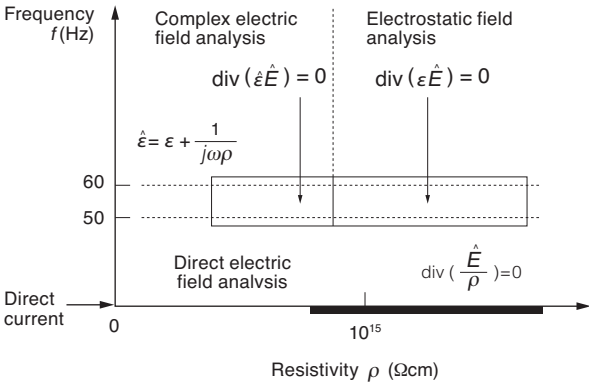

Fig. 4. Types and application range of electric field analysis

An example of the electric field analysis of oil-immersed termination sealing ends is shown in **Fig. 5**. One type of electric cable termination is an oil-immersed sealed end. This is comprised of a cable insulator (crosslinked polyethylene) to which a stress cone (a component capable of adjusting electric fields by combining insulating rubber and conducting rubber) and insulator (epoxy) are attached so that the interface between the stress cone and insulator is placed under constant pressure. It is an axisymmetric three-dimensional structure created by revolution around the z axis. The results of electrostatic field analysis, in which each insulator's relative permittivity is given, are shown in **Fig. 6** (equipotential lines), **Fig. 7** (maximum electric field), and **Fig. 8** (electric field distribution of insulator interface).

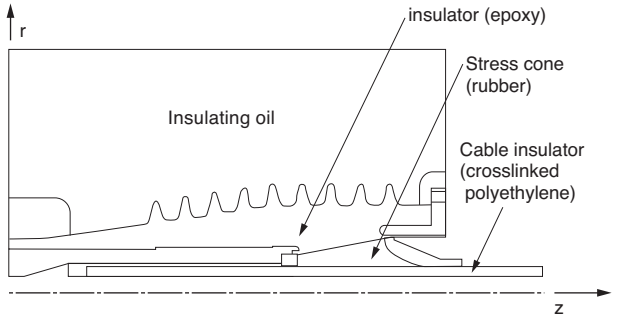

Fig. 5. Electric field analysis model (oil-immersed termination sealing end)

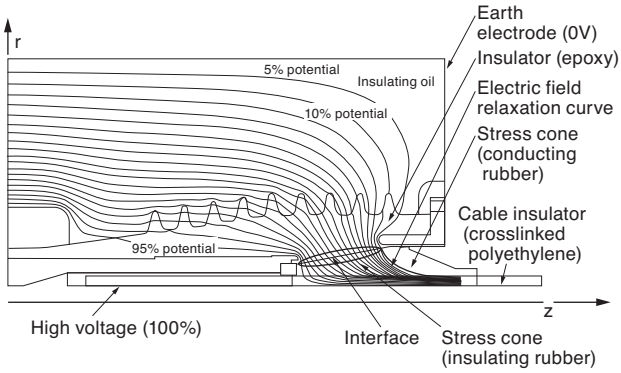

Fig. 6. Equipotential lines

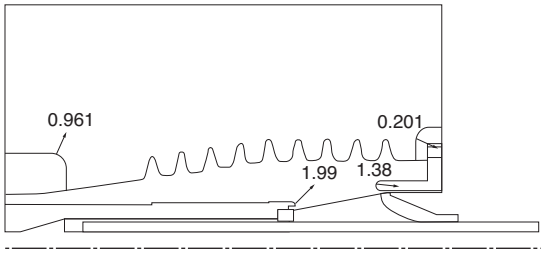

Fig. 7. Maximum electric field(%/mm)

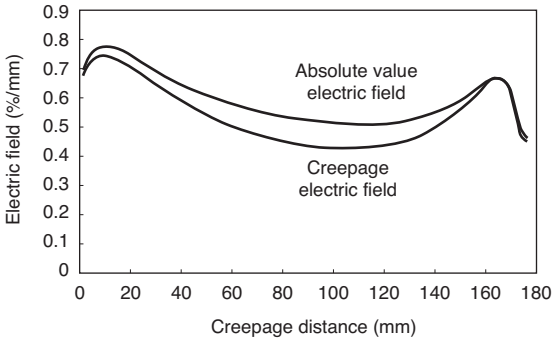

Fig. 8. Electric field distribution on the insulator interface

4. Magnetic Field Analysis

4-1 Purpose of Magnetic Field Analysis

When an electric current flows, a magnetic flux occurs around it. In order to allow the magnetic flux to pass through, a magnetic circuit made from magnetic materials, such as electrical steel sheet, electromagnetic soft iron, or permalloy, is used. When the current intensity increases, a region may be created where the magnetic flux of the magnetic materials does not increase proportionately, a condition called magnetic saturation. It is therefore necessary to conduct nonlinear analysis to take into account the B-H curve of the magnetic material. Magnetic field analysis is conducted for the design of magnetic circuits, e.g., to find the cross-sectional shape required for a

magnetic material so that magnetic flux will pass through without its being saturated.

When a magnetic field penetrating a conductor fluctuates, an eddy current flows in the conductor. If magnetic field analysis is conducted with this taken into account, impedance can be discovered by calculating the current distribution in the section of a conductor through which alternating current passes.

4-2 Current Sensor Analysis via Magnetic Field Analysis

Shown in **Fig. 9** is an example of the magnetostatic analysis of a current sensor. An open-loop current sensor consists of a magnetic core with a gap, a Hall element, and a circuit that amplifies output from the Hall element. The current flowing through the conductor that passes the core generates a magnetic flux in proportion to the current at the gap. The Hall element then converts this magnetic flux into voltage signals. The output voltage from this Hall element is amplified by the amplifier circuit, thereby generating output voltage in proportion to the measured current.

Fig. 10 shows the B-H curve of PC permalloy that was used in the magnetic core, while **Fig. 11** shows the analysis results of the magnetic core's magnetic flux density distribution. Using the magnetic flux density distribution, the saturation status of the magnetic core may be investi-

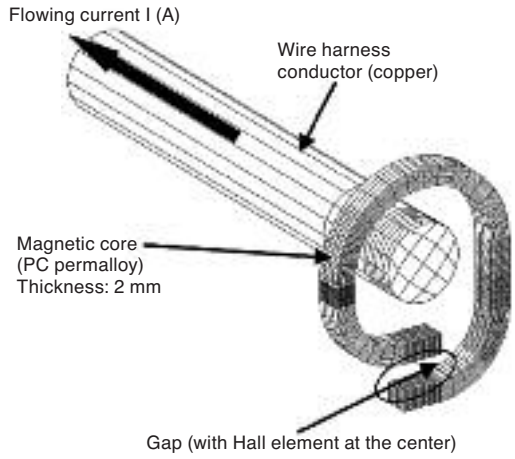

Fig. 9. Structure of the current sensor

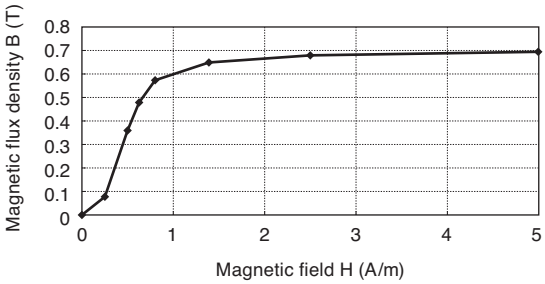

Fig. 10. B-H curve of Magnetic core (PC permalloy)

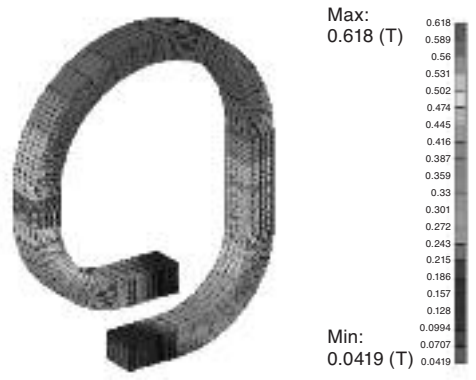

Fig. 11. Magnetic core's magnetic flux density distribution (thickness: 2 mm, I = 100 A)

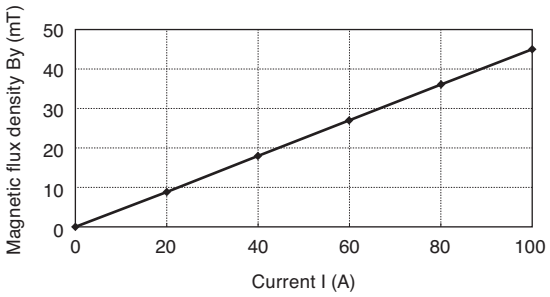

Fig. 12. Flowing current and magnetic flux density at the gap (core thickness: 2 mm)

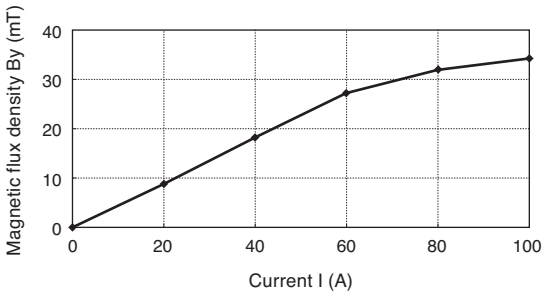

Fig. 13. Flowing current and magnetic flux density at the gap (core thickness: 1 mm)

gated. It was confirmed that, using a 2 mm thick magnetic core, magnetic flux density at the gap was proportional to an electric current of up to 100 A, and thus may be used as a current sensor (**Fig. 12**). When a 1 mm thick magnetic core was used, however, the magnetic flux density at the gap was not proportional to the flowing current once it exceeded 60 A, which would be inappropriate in a current sensor (**Fig. 13**).

4-3 Current Distribution / Impedance Analysis via Magnetic Field Analysis

As an example of eddy current analysis, the current distribution in the conductor's cross section and the high frequency impedance with single- and three-phase cur-

rent applied to the conductor's transmission line with a circular and rectangular cross section are shown below [27]. This analysis was made because the frequency of the motor current for driving electric vehicles is in the kHz range, so that high-frequency effects occur (skin effect, proximity effect).

Using the finite element method, magnetic field analysis was conducted with eddy currents on a single-core right cylindrical conductor. The analysis found that current distribution and impedance agreed with theoretical values, leading us to believe that accurate impedance analysis can be carried out by magnetic field analysis. Then, current distribution was analyzed when single- and three-phase currents were applied to a right cylindrical conductor and a conductor with a rectangular cross section, to obtain impedance (resistance, inductance).

(1) Impedance of a Single-core Right Cylindrical Conductor

Current density distribution in the radial direction r and the conductor's impedance were analyzed for the case in which voltage was applied to both end surfaces in the longitudinal direction z of a single-core right cylindrical conductor (**Fig. 14**). Assuming an aluminum conductor (conductivity $\sigma = 3.31 \times 10^7$ S/m), $a = 5$[mm], $\ell = 1$[m], $V = 1$[V], and $f = 1,10$[kHz], finite element method based magnetic field analysis was carried out for eddy currents in the frequency domain in order to obtain the current distribution. Illustrated by dots in **Fig. 15** is the distribution of current density in the radial direction $i\,(r)/i\,(a)$, which was normalized by current density $i\,(a)$ on the conductor's surface (r = a). Also shown with lines in **Fig. 15** are the theoretical values of current density distribution.

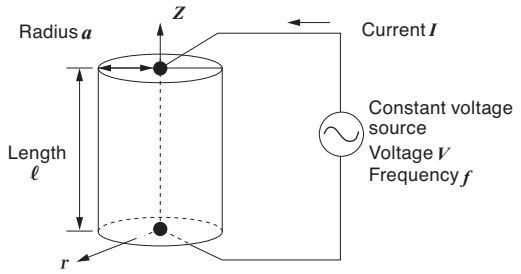

Fig. 14. Single-core right cylindrical conductor

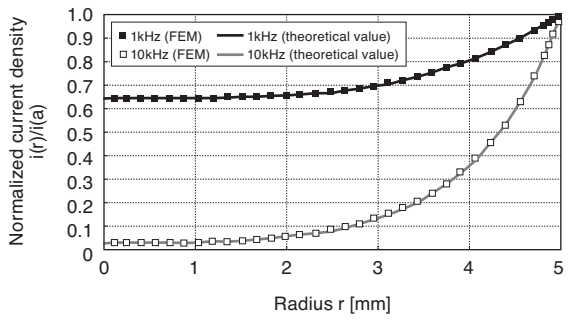

Fig. 15. Current density distribution of a single-core right cylindrical conductor

Table 4 compares the impedance obtained by magnetic field analysis and the theoretical values of impedance.

As shown in **Fig. 15**, due to the skin effect, the current density on the conductor's surface is high, which becomes more conspicuous as frequency increases. Based on the data given in **Fig. 15** and **Table 4**, it can be gathered that the magnetic field's analysis result values agree closely with the theoretical values, thus leading to the conclusion that impedance may be obtained accurately through magnetic field analysis.

Table 4. Impedance of a single-core right cylindrical conductor

	Resistance (mΩ)		Self-inductance (μH)	
f (kHz)	1	10	1	10
Theoretical value	0.464	1.203	1.049	1.049
Analysis result	0.458	1.205	1.119	1.091

f: Frequency DC resistance: 0.385 (mΩ)

(2) Impedance of a Parallel Conductor with a Rectangular Cross Section

Using parallel conductors with rectangular cross sections (see **Fig. 16**), magnetic field analysis was conducted to find current distribution and impedance, assuming an aluminum conductor (conductivity $\sigma = 3.31 \times 10^7$ S/m), $a = 10$[mm], $b = 2$[mm], $d = 1$[mm], $\ell = 1$[m], $V = 1$[V], and $f = 1,10$[kHz].

Shown in **Fig. 17** is the current distribution of the conductors' cross section in the case of serial connection. In this case, due to skin and proximity effects, the current density is high at both edges on the counter-face surfaces of the conductor. The higher this frequency is, the more conspicuous this tendency becomes.

In the case of serial connection, the conductors' impedance was calculated by varying the gap d from 1 mm, to 5 mm, and then to 9 mm [27]. Magnetic field analysis made it possible to calculate the impedance of a conductor with a rectangular cross section.

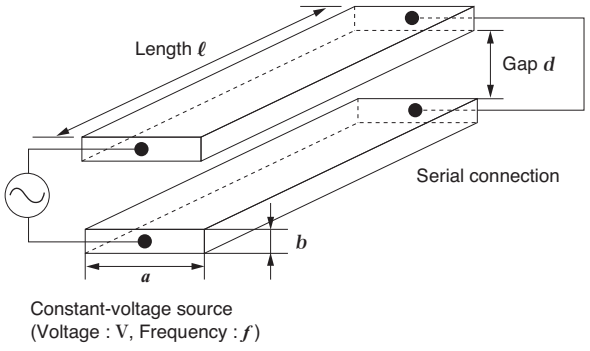

Fig. 16. Parallel conductor with a rectangular cross section

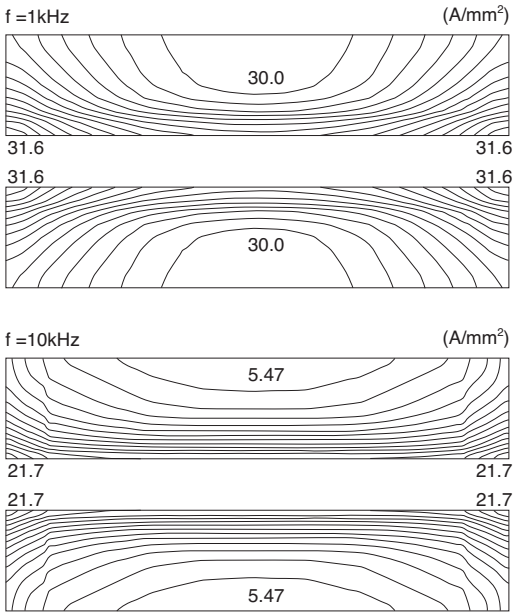

Fig. 17. Current density distribution of a parallel conductor with a rectangular cross section (serially-connected)

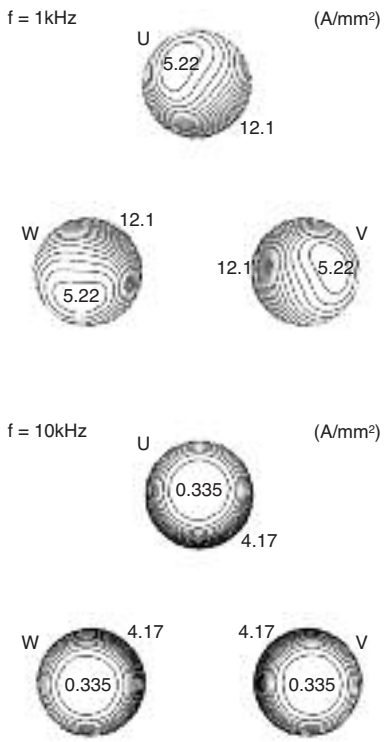

Fig. 19. Current density distribution of right cylindrical conductors arranged in a regular triangular shape (three-phase)

(3) Impedance of a Three-phase Conductor

As shown in **Fig. 18**, three right cylindrical conductors were arranged in a regular triangular shape, and the magnetic field was analyzed when a three-phase voltage was applied. Assuming an aluminum conductor (conductivity $\sigma = 3.31 \times 10^7$ S/m), $a = 5$[mm], $d = 20$[mm], $\ell = 1$[m], $V = 1$[V], and $f = 1,10$[kHz], magnetic field analysis was conducted in order to obtain current distribution and impedance.

The current distribution in the conductors' cross sections is shown in **Fig. 19**. Due to skin and proximity effects, a high current density is observed at some points on the counter-face surfaces of the conductors. The current distribution patterns of each phase are identical, overlapping each other if rotated by 120°. Shown in **Table 5** are the analysis results for the conductor's impedance. The values for each phase are identical, creating an impedance of three-phase equilibrium.

Table 5. Impedance of right cylindrical conductors arranged in a regular triangular shape (three-phase)

Frequency f (kHz)	Resistance (mΩ)	Inductance (μH)	Impedance (mΩ)
1	0.503	0.314	2.03
10	1.40	0.278	17.6

DC resistance: 0.385 (mΩ)

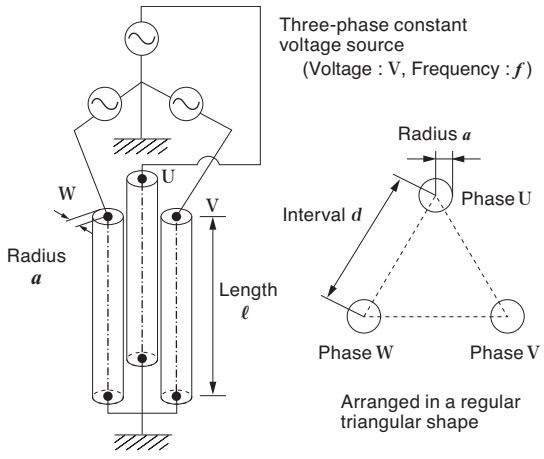

Fig. 18. Right cylindrical conductors arranged in a regular triangular shape (three-phase)

Analysis results for a conductor with a rectangular cross section can be found in Reference [27].

5. Future Outlook

Electromagnetic analysis, for which both electric and magnetic fields must be found, is typically used for evaluating the electromagnetic compatibility (EMC) of wire harnesses for automobiles and signal integrity (SI) such as the transmission characteristics of high-frequency products, and for analysis of high-frequency components' impedance-frequency characteristic. Application of electro magnetic field analysis is expected to extend to product design and development and quality assurance.

Concerning electric field analysis and magnetic field analysis, in an increasing number of cases designers are

using CAD drawing data to conduct finite-element based discretization and analysis. Accordingly, efforts are under way to develop technologies for a designer-friendly system.

6. Conclusion

Analyses of electric and magnetic fields were explained and demonstrated with example procedures performed at Sumitomo Electric. Going forward, the author wishes to address some existing issues, including the need to develop a designer-friendly electromagnetic analysis system. The author also wishes to make continued efforts to develop electromagnetic analysis techniques that are useful in product development and to conduct electromagnetic field analysis using large-scale models.

References

(1) "Present State of Finite Element Method Based Electromagnetic Field Analysis of Power Equipment," The Institute of Electrical Engineers of Japan (IEEJ) Technical Report, Part II, No. 118, 1981
(2) "Applying the Electromagnetic Numerical Analysis Method to Power Equipment," IEEJ Technical Report, Part II, No. 208, 1986
(3) "Three-dimensional Magnetostatic Field Numerical Calculation Techniques," IEEJ Technical Report, Part II, No. 286, 1988
(4) "Electromagnetic Field Numerical Analysis Method for Rotating Machines," IEEJ Technical Report, Part II, No. 375, 1991
(5) "Three-dimensional Eddy Current Field Numerical Calculation Techniques," IEEJ Technical Report, Part II, No. 384, 1991
(6) "Practical Techniques for Three-dimensional Electromagnetic Field Numerical Calculation," IEEJ Technical Report, No. 480, 1994
(7) "Applied Electromagnetic Field Analysis Software Techniques for Rotating Machines," IEEJ Technical Report, No. 486, 1994
(8) "Electromagnetic Field High Precision Numerical Simulation Techniques for Rotating Machines," IEEJ Technical Report, No. 565, 1995
(9) "Electromagnetic Analysis and its Application to its Inverse Optimization Problems," IEEJ Technical Report, No. 611, 1996
(10) "Present State and Examples of Practical Techniques for Electromagnetic Field Analysis of Rotating Machines," IEEJ Technical Report, No. 663, 1998
(11) "Advancement of Electromagnetic Field Analysis Techniques and Optimization Techniques," IEEJ Technical Report, No. 759, 1999
(12) "Electromagnetic Field Analysis Techniques for Virtual Engineering of Rotating Machines," IEEJ Technical Report, No. 776, 2000
(13) "Electromagnetic Field Analysis Techniques for Three-dimensional CAE of Rotating Machines," IEEJ Technical Report, No. 855, 2001
(14) "Recent Technological Trends in Electromagnetic Field Numerical Analysis," IEEJ Technical Report, No. 906, 2002
(15) "High-speed and large-scale computation in electromagnetic analysis," IEEJ Technical Report, No. 1043, 2006
(16) "Advanced computational techniques for practical electromagnetic-field analysis," IEEJ Technical Report, No. 1129, 2008
(17) Teruya Kono, Makoto Katsurai, "Practical Study of Electromagnetics," pp.159-160, p.175, IEEJ, 1978
(18) Takayoshi Nakata, Norio Takahashi, "Finite Element Method for Electrical Engineering 2nd Edition," Morikita Publishing Co., Ltd., 1982
(19) The Japan Society of Applied Electromagnetics and Mechanics (JSAEM), "Basics of Numerical Electromagnetic Field Analysis Methods," written and edited by Hajime Tsuboi and Tadashi Naitoh, Yokendo Co., Ltd., 1994
(20) JSAEM, "Practical Numerical Electromagnetic Field Analysis Methods," written and edited by Hajime Tsuboi and Tadashi Naitoh, Yokendo Co., Ltd., 1995
(21) "High Voltage Test Methods for CV Cables and Cable Joints or Ends," Electric Technology Research, Vol. 51, No. 1, pp.53-55, 1995
(22) "New Edition – Power Cable Technology Handbook," supervised by Kihachiro Iizuka, Denkishoin Co., Ltd., pp.395-424, 1989
(23) Toshiyuki Inoue, Yuichi Maekawa, Hiroshi Suzuki, Kohei Furukawa, Ryosuke Hata, Kaihei Murakami,Munehisa Mitani, Hiroyuki Kimura, Hiroshi Hirota, Yoshihisa Asao, Yuichi Ashibe, Morihiro Seki, "Construction of Direct Current 500 kV PPLP Insulating OF Submarine Cable Lines," SEI Technical Review, No. 155, pp.69-76, 1999
(24) Kaoru Takuma, Shoji Hamada, "Basics and Applications of Numerical Electric Field Calculation," Tokyo Denki University Press, pp.196-197, 2006
(25) "New Edition – Power Cable Technology Handbook," supervised by Kihachiro Iizuka, Denkishoin Co., Ltd., pp.81-100, 1989
(26) "Electric Wire Engineering Data: Electric Power, Insulated Wires," SEI, p.872, 1990
(27) Tomohiro Keishi, Toshirou Shimada, Yoshio Mizutani, "A Consideration of High-frequency Effects on Power Harnesses Used in Electric Vehicles (1)," The Papers of Joint Technical Meeting on Static Apparatus and Rotating Machinery, IEE Japan, SA-09-19/RM-09-19, 2009

(References are all written in Japanese.)

Contributor

T. KEISHI
• Senior Specialist
Dr. Engineering
Manager, CAE Solution Group, Analysis Technology Research Center
Involved in research of Computer Aided Engineering (CAE)